Specificity Modulation of Barley α-Amylase through Biased Random Mutagenesis Involving a Conserved Tripeptide in $\beta \rightarrow \alpha$ Loop 7 of the Catalytic $(\beta/\alpha)_8$-Barrel Domain†

Tine E. Gottschalk,‡,§ Dedreia Tull,‡,|| Nushin Aghajari,⊥ Richard Haser,⊥ and Birte Svensson*,‡

Department of Chemistry, Carlsberg Laboratory, Gamle Carlsberg Vej 10, DK-2500 Copenhagen Valby, Denmark, and Institut de Biologie et Chimie des Protéines, Laboratoire de Bio-Cristallographie, UMR 5086, CNRS and Université Claude Bernard Lyon 1, 7 Passage du Vercors, 69367 Lyon cedex 07, France

Received April 26, 2001; Revised Manuscript Received July 12, 2001

ABSTRACT: The relative specificity and bond cleavage pattern of barley α-amylase 1 (AMY1) were dramatically changed by mutation in F^{286}VD that connected β-strand 7 of the catalytic $(\beta/\alpha)_8$-barrel to a succeeding 3_{10}-helix. This conserved tripeptide of the otherwise variable $\beta \rightarrow \alpha$ segment 7 lacked direct ligand contact, but the nearby residues His290 and Asp291 participated in transition-state stabilization and catalysis. On the basis of sequences of glycoside hydrolase family 13, a biased random mutagenesis protocol was designed which encoded 174 putative F^{286}VD variants of C95A-AMY1, chosen as the parent enzyme to avoid inactivating glutathionylation by the yeast host. The FVG, FGG, YVD, LLD, and FLE mutants showed 12−380 and 1.8−33% catalytic efficiency (k_{cat}/K_m) toward 2-chloro-4-nitrophenyl β-D-maltoheptaoside and amylose DP17, respectively, and 0.5−50% activity for insoluble starch compared to that of C95A-AMY1. K_m and k_{cat} were decreased 2−9- and 1.3−83-fold, respectively, for the soluble substrates. The starch:oligosaccharide and amylose:oligosaccharide specificity ratios were 13−172 and 2.4−14 for mutants and 520 and 27 for C95A-AMY1, respectively. The FVG mutant released 4-nitrophenyl α-D-maltotrioside ($PNPG_3$) from $PNPG_5$, whereas C95A-AMY1 produced PNPG and $PNPG_2$. The mutation thus favored interaction with the substrate aglycon part, while products from $PNPG_6$ reflected the fact that the mutation restored binding at subsite −6 which was lost in C95A-AMY1. The outcome of this combined irrational and rational protein engineering approach was evaluated considering structural accommodation of mutant side chains. FVG and FGG, present in the most active variants, represented novel sequences. This emphasized the worth of random mutagenesis and launched flexibility as a goal for $\beta \rightarrow \alpha$ loop 7 engineering in family 13.

α-Amylases (α-1,4-D-glucan glucanohydrolase, EC 3.2.1.1) hydrolyze internal α-1,4-glucosidic bonds in starch, maltodextrins, and maltooligosaccharides (*1*). Cereal α-amylases are essential in brewing and baking, and microbial enzymes find widespread application in the starch and food industries. There has been great interest in modifying the specificity of α-amylases and other important enzymes of glycoside hydrolase family 13 (*2*−*4*). However, despite substantial structure information, sufficient insight into features critical for specificity lags behind. As a consequence, few examples, mainly for cyclodextrin glycosyltransferases (*5*, *6*), have been reported of designer enzymes having altered specificity along with a suitable level of activity. In the work presented here, a biased random mutagenesis strategy was used to modify substrate specificity and product profiles of barley α-amylase 1 (AMY1).[1] In contrast to the major AMY2 isozyme from germinating seeds or malt (*7*, *8*), the minor AMY1 (*7*, *9*) can also be readily obtained by heterologous expression in yeast (*10*−*13*) and is currently developed using protein engineering (*14*−*16*). The sequences of the two isozymes are 80% identical, but they have distinctly different enzymic and stability properties (*7*−*9*, *17*).

The active site of AMY1 contains 10 consecutive subsites accommodating substrate glucosyl residues (*18*), i.e., subsites −1 through −6 toward the nonreducing end and subsites 1−4 toward the reducing end of the substrate. Various other α-amylases contain 5−11 subsites (*19*, *20*). The three-dimensional structures of free AMY2 and of AMY2 in complex with acarbose, a pseudotetrasaccharide inhibitor, are available (*21*, *22*). It consists of a $(\beta/\alpha)_8$-barrel (domain A), a small domain B protruding between the third β-strand and α-helix of the $(\beta/\alpha)_8$-fold, and a C-terminal five-stranded antiparallel β-sheet (domain C). Domains A and B participate in substrate binding and catalysis (*13*, *21*, *23*, *24*). Structures

† This work was supported by the EU Third and Fourth Framework Programmes on Biotechnology (CT94-3008 and CT98-0022).

* To whom correspondence should be addressed. Phone: +45 33 27 53 45. Fax: +45 33 27 47 08. E-mail: bis@crc.dk.

‡ Carlsberg Laboratory.

§ Present address: Pharmexa, Kogle Allé 6, DK-2970 Hørsholm, Denmark.

|| Present address: Department of Biochemistry and Molecular Biology, University of Melbourne, Parkville 3052, Victoria, Australia.

⊥ CNRS and Université Claude Bernard Lyon 1.

[1] Abbreviations: AMY1 and AMY2, barley α-amylases 1 and 2, respectively; Cl-$PNPG_7$, 2-chloro-4-nitrophenyl β-D-maltoheptaoside; PNP, 4-nitrophenol; PNPG, 4-nitrophenyl α-D-glucoside; $PNPG_2$, 4-nitrophenyl α-D-maltoside; $PNPG_3$−$PNPG_7$, 4-nitrophenyl α-D-maltotrioside through 4-nitrophenyl α-D-maltoheptaoside, respectively.

10.1021/bi0108608 CCC: $20.00
Published on Web 10/04/2001

of free or complexed α-amylases from *Aspergillus oryzae* (Taka-amylase A; *25*, *26*), *Aspergillus niger* (*27*), porcine pancreas (*28*, *29*), human salivary glands (*30*) and pancreas (*31*), yellow meal worm (*32*), *Bacillus licheniformis* (*33*), *Bacillus subtilis* (*34*), *Bacillus stearothermophilus* (*35*), and *Pseudoalteromonas haloplanktis* (*36*) are also available. Recently, the structure of a chimeric *Bacillus* α-amylase with a bound decasaccharide analogue was determined (*20*). Glycoside hydrolase family 13 currently comprises 26 specificities (*2*, *4*, *37*), and structures of cyclodextrin glycosyltransferase (*38*, *39*), oligo-1,6-glucosidase (*40*), maltotetraohydrolase (*41*), isoamylase (*42*), TVA II α-amylase (*43*), cyclodextrinase (*44*), amylomaltase (*45*), glycosyltrehalose trehalohydrolase (*46*), and amylosucrase (*47*) have been reported. Selected family members in this study defined the mutant gene pool and were used to discuss the results of the mutagenesis with the focus on heterologous protein production and enzymic properties of the mutant enzymes.

Insight into the mechanism and substrate interactions at the long binding site was gained from structures of complexes of (i) substrates with inactive mutants of α-amylase (*34*, *48*), cyclodextrin glycosyltransferase (*39*, *49*, *50*), and maltotetraohydrolase (*51*), (ii) active enzymes and inhibitory maltooligosaccharide analogues (*20*, *21*, *26*, *28*, *35*, *49*, *50*, *52*), and (iii) substrate docking in α-amylases (*24*, *53*). Throughout the binding crevice sugar rings stacking onto aromatic side chains and hydroxyl groups are forming hydrogen bonds with the protein and with structural water molecules. The three catalytic residues (Asp180, Glu205, and Asp291 in barley AMY1) are situated at C-terminal extensions of β-strands 4, 5, and 7 in the $(\beta/\alpha)_8$-fold (*4*, *21*). Structure overlays (*44*, *54*) revealed numerous differences for most of the eight $\beta \rightarrow \alpha$ segments that created the extended active site on the C-terminal side of the $(\beta/\alpha)_8$-barrel, while the three catalytic acids from different family members did superimpose perfectly (*34*, *42*). Variation in the $\beta \rightarrow \alpha$ segments has been correlated with specificity differences. Characteristic sequence motifs and side chains are thus connected with, for example, hydrolysis and transglycosylation involving α-1,4 versus α-1,6 linkages (*2*, *4*, *40*, *42*, *43*, *55*, *56*).

This work focuses on $\beta \rightarrow \alpha$ segment 7 that in its C-terminal part displays conspicuous diversity in length, shape, and extrabarrel secondary structures. His305 from this stretch in mammalian enzymes undergoes a major conformational rearrangement that is concomitant with oligosaccharide binding (*28*, *29*). For the present mutational manipulation of enzymic properties, the preferred target in AMY1 was a conserved tripeptide ($F^{286}VD$) from the N-terminal part of $\beta \rightarrow \alpha$ segment 7 as modification in the highly variable C-terminal part was considered risky. Earlier structure−function relationship investigations in AMY1 by site-directed mutagenesis and protein engineering (*13*−*16*, *23*, *45*, *57*, *58*) reflected considerable tolerance to amino acid substitution which encouraged further mutagenesis in AMY1. For structural reasons, however, biased random mutagenesis was applied in the case of the present target, as the conserved $F^{286}VD$ sequence may be critical for activity and conformational stability (*21*, *22*). The resulting $F^{286}VD$ mutants offer a wide range of changes in enzymic properties and put forward increased flexibility of $\beta \rightarrow \alpha$ loops as a possible general goal for protein engineering in family 13. C95A-AMY1 was chosen as a parent to avoid inactivating glutathionylation of Cys95 by the host organism (*11*, *14*).

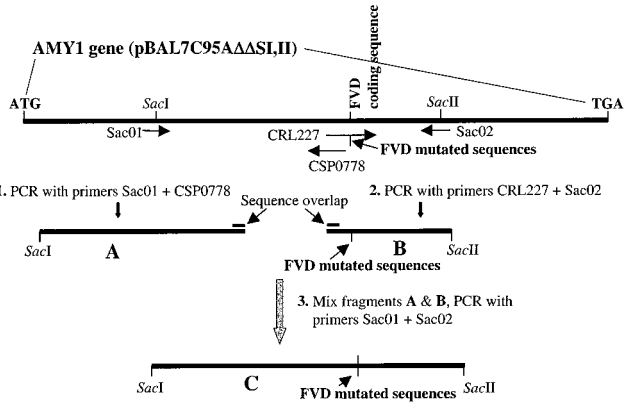

FIGURE 1: Construction of PCR-amplified DNA fragments containing biased randomly mutated sequences of the $F^{286}VD$ encoding region (see the text for details).

MATERIALS AND METHODS

Strains and Plasmids. *Escherichia coli* DH5α was used to propagate pBAL7C95AΔSI,II that contains the insert encoding C95A-AMY1 (*14*) and carries the LEU2 marker gene for selection of *Saccharomyces cerevisiae* transformants. Heterologous gene expression in *S. cerevisiae* JHRY20-2C (ATCC 96713) was driven by the PGK promoter (*10*). Silent mutations of the C95A-AMY1 gene removed *Sac*II and *Sac*I sites at positions 471 and 646 (*14*), making the remaining unique *Sac*I and *Sac*II sites useful for subcloning. Cys95 was mutated to Ala to avoid inactivating glutathionylation of this specific free thiol group by the yeast hosts (*11*, *12*, *14*). *Pichia pastoris* GS115 (Invitrogen) was used for expression of mutant genes inserted in pHIL-D2 (Invitrogen) as described previously (*12*). Standard growth media were used for *S. cerevisiae* (*14*) and *P. pastoris* (*12*).

Biased Random Mutagenesis. Standard cloning techniques were used throughout (*59*, *60*). Biased random mutagenesis of the $F^{286}VD$ encoding sequence in pBAL7C95AΔSI,II was performed using overlapping oligonucleotides encoding F^{286}-VD mutants, extended by PCR to full-length fragments (Figure 1). Two AMY1 gene fragments (A and B) were PCR amplified, of which B carried the $F^{286}VD$ mutant gene pool. The A and B products were fused by PCR overlap extension using primers between the 3′- and 5′-ends of A and B, respectively. Product C of 1018 bp contained a mixture of mutated $F^{286}VD$ encoding sequences (Figure 1). Primers were as follows: Sac01 5′-primer, 5′-TTTTT GAG CTC AAG TCG CTC ATC GGC (position 375); CSP0778, 5′-GGT GGC GGC CTT GGC CGG (position 1023); CRL227, 5′-CCG GCC AAG GCC GCC ACC [T(67%)/C(33%) T(67%)/A(33%) C(67%)/G(33%)] [C(33%)/G(33%)/T(33%) T(67%)/G(33%) G] [G(67%)/A(33%) A(67%)/G(33%) C(67%)/G(33%)] AAC CAC GAT ACA GGC (position 1006); Sac02 3′-primer, 5′-TTTTT CCG CGG CAC CGT TCT TCT CCC (position 1393); they enabled 174 combinations of amino acids at AMY1 positions 286−288 (Table 1). Standard PCR consisted of 30 cycles of 1 min at 94 °C, 1 min at 55 °C, and 2 min at 72 °C; overlap extension PCR had four cycles of 2 min at 94 °C, 2 min at 38 °C, and 3 min at 72 °C, followed by 30 standard PCR cycles. The product C mixture

Table 1: Putative Substitution in the $F^{286}VD$ Sequence of C95A-AMY1 Encoded by Designed Biased Random Mutations

wild type	encoded mutant residues
Phe286	Phe, Leu, Tyr, His, Gln (amber-STOP)
Val287	Val, Arg, Gly, Leu, Trp
Asp288	Asp, Glu, Gly, Asn, Lys, Arg, Ser

was purified (Ultrafree MC; Pharmacia), subcloned in pBAL7C95AΔSI,II at *Sac*I and *Sac*II to yield npBAL7C95AΔSI,II, and used for *E. coli* transformation. Single *E. coli* transformant colonies from agar plates were grown overnight in 5 mL of LB/Amp (50 μg/mL); plasmids were purified (Plasmid Kit, Qiagen, Hilden, Germany), and the mutations were identified by DNA sequencing (Applied Biosystems 373A DNA sequencer; Taq DyeDeoxy Terminator Cycle Sequencing kit; Perkin-Elmer).

S. cerevisiae JHRY20-2C (*10*, *14*) was transformed by npBAL7C95AΔSI,II using a lithium acetate method (*60*, *61*) and screened on starch plates developed by exposure to I_2 vapor (*62*). Because too little activity, however, was secreted for reliable identification of useful transformants, *S. cerevisiae* JHRY20-2C was subsequently individually transformed by 21 yeast expression plasmids encoding different $F^{286}VD$ mutants identified by sequencing 100 clones isolated from *E. coli* (see above). Later, *P. pastoris* GS115 was transformed by electroporation using expression plasmids containing selected mutant genes, which had been constructed by PCR amplification using primers for insertion into pHIL-D2 at the unique *Eco*RI site between the AOX promoter and terminator (*12*). His^+, $Mut^÷$ (methanol utilization deficient) transformants were selected on $His^÷$ plates followed by plates with methanol as the sole carbon source for identifying $Mut^÷$ colonies that monitored integration at the genomic AOX site. These transformants were tested for secretion of the active enzyme on plates containing starch and methanol.

Enzyme Production. S. cerevisiae transformants harboring $F^{286}VD$ mutant genes (Table 2) were grown (MBR BioReactor) for 3 days in 10 L of SD-Leu medium at 25 °C. Then fresh glucose was added to a final concentration of 2%; the fermentation was continued for 3 days, and the supernatant was recovered by centrifugation and concentrated to 400 mL (Pellicon unit; polyethersulfone membranes; 30 kDa cutoff; Millipore). To test for secretion of AMY1 variants, culture aliquots were removed during growth, concentrated 10−30-fold (Centricon, 10 kDa cutoff; Amicon) to exceed the detection limit of 100 pg of AMY1, corresponding to approximately 20 μg/L of culture, and 5 μL was applied for immuno-dot blotting on nitrocellulose (Schleicher & Schuell, Dassel, Germany) standardized by 0.125−125 ng of rAMY1 and developed using rabbit anti-AMY2 immune serum diluted 1:750 essentially as described previously (*14*).

$F^{286}VD$ mutants were purified from concentrated culture supernatants by affinity chromatography on β-cyclodextrin-Sepharose (*10*, *12*, *14*) and analyzed (40−360 ng) essentially as described previously (*14*, *62*) by IEF (PhastGel, pI 4−6.5; Phast-System, Pharmacia), as visualized by silver staining and in a zymogram by soaking with a starch followed by a KI/I_2 solution (*62*), and by SDS−PAGE (PhastGel, 10 to 15%) and Western blotting (ProtoBlot Western Blot AP System, Promega, Madison, WI; anti-AMY2 immune serum diluted 750-fold). Enzyme concentrations were calculated from the amino acid contents of protein (100 ng) hydrolysates (Alpha Plus amino acid analyzer; OPA detection; Pharmacia), and secretion levels were assessed from the amounts of purified enzymes. Parent C95A-AMY1 was prepared from *S. cerevisiae* (*14*). Fermentation of *P. pastoris* and production of wild-type rAMY1 in *P. pastoris* were carried out essentially as described previously (*12*).

Activity Assays. *(1) Insoluble Blue Starch*. One "Phadebas Amylase Test 100" tablet (Pharmacia) in 20 mM sodium acetate and 1 mM $CaCl_2$ (pH 5.5, 4 mL) was added to the mutant or reference enzyme to a final concentration of $1-10^2$ or 1.1−2.2 nM and the mixture incubated for 15 min at 37 °C. The reaction was stopped by 0.5 M NaOH (1 mL); aliquots (1 mL) were centrifuged, and the supernatants (300 μL) were transferred to a microtiter plate for A_{620} reading (Ceres UV900 HDI microplate reader, Biotek Instruments, Inc.). Alternatively, 6.25 mg/mL insoluble Blue Starch (customer preparation, Pharmacia) was used in the above buffer with 0.05% BSA (*14*). One unit corresponds to the amount of enzyme giving a ΔA_{620} of 0.001 in 15 min in the final volume (5 mL).

(2) Amylose. Amylose DP17 (Hayashibara Chemical Laboratories, Okayama, Japan) hydrolysis in 20 mM sodium acetate, 5 mM $CaCl_2$ (pH 5.5), and 0.05% BSA at 37 °C by 14.0−87.5 nM mutant or 5.0 nM reference enzyme was assessed on aliquots removed over a 2−10 min interval by determination of the amount of reducing sugar using copper bicinchoninate and maltose as standards (*14*, *63*). The samples were boiled and transferred to microtiter plates (3 × 300 μL) for A_{540} reading. k_{cat} and K_m were calculated (Enzfitter, Biosoft) from initial rates at eight substrate concentrations (0.10−6.66 mg/mL).

(3) 2-Chloro-4-nitrophenyl β-D-Maltoheptaoside. The rate of hydrolysis of 2-chloro-4-nitrophenyl β-D-maltoheptaoside (Cl-$PNPG_7$) (Granutest 3, Merck, Darmstadt, Germany) at 30 °C was determined (*14*) using 7.4−67.0 nM enzyme. k_{cat} and K_m were calculated as described above from initial rates at 10 substrate concentrations (0.20−13.0 mM).

Bond Cleavage Frequencies. 4-Nitrophenyl α-D-maltopentaoside ($PNPG_5$), $PNPG_6$ (Calbiochem, Bad Soden, Germany), or $PNPG_7$ (Boehringer Mannheim, Mannheim, Germany), each at 1 mM, in 20 mM sodium acetate (pH 5.5, 250 μL) was hydrolyzed by 80−280 nM enzyme at 37 °C. The reaction was stopped by adding 10% CH_3COOH (10 μL) to aliquots (50 μL) during the interval from 15 s to 15 min. Products and substrate were separated on a Bio-Sil Disaccharide column (4 × 250 mm; Amino 5S; Bio-Rad) thermostated at 37 °C and eluted by 75% CH_3CN (aq) at a rate of 0.7 mL/min using a Waters HPLC model 510 pump. 4-Nitrophenol, PNPG, and $PNPG_2$−$PNPG_7$ were quantified at 313 nm (Shimadzu SPD-10AU UV−vis detector) using standard mixtures (0.05−1 mM). K_m was ≥10 mM as estimated from the initial rates of hydrolysis at four concentrations of $PNPG_7$ and $PNPG_6$.

Molecular Graphics Structure Comparison and Structure-Based Evaluation of Mutant Properties. Structures from the Protein Data Bank (*64*) were displayed and compared using TURBO-FRODO (*65*), which was applied also for in silico mutation. Superposition of C_α backbones was performed using the "rigid" option, and the C_α atoms of the three catalytic acids were used to make a rough rigid-body fit. Taking these new positions as a starting point, we carried

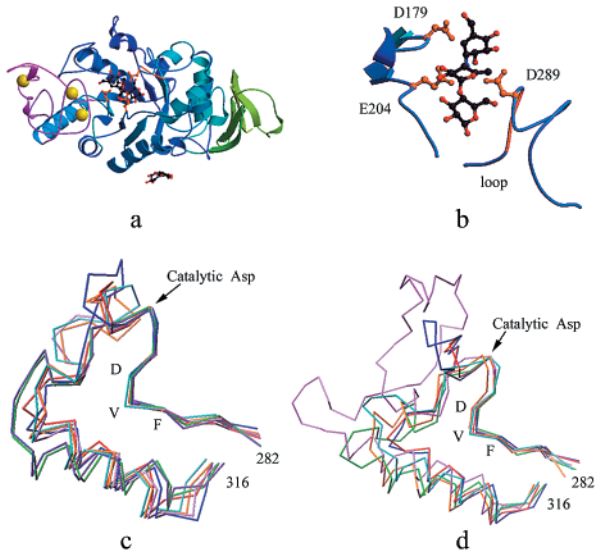

FIGURE 2: Molecular structure of barley α-amylase 2/acarbose (*21*). (a) Global structure of AMY2 highlighting the $F^{284}VD$ segment (orange), the catalytic acids [Asp179, Glu204, and Asp289 (orange)], three rings of acarbose occupying subsites −1, 1, and 2, and a disaccharide unit (in black) at the surface site. Domain A is colored in blue, domain B in magenta, and domain C in green. Calciums 500, 501, and 502 (*22*) are shown as yellow spheres. (b) Closeup of acarbose at the active site. FVD in $\beta \rightarrow \alpha$ segment 7 and catalytic acids in orange (AMY2 numbering). (c) Superposition of β-strand 7 through α-helix 7 of the $(\beta/\alpha)_8$-barrel domain from seven α-amylases: barley AMY2 (red), *A. oryzae* (purple), *A. niger* (green), *Ps. haloplanktis* (light blue), *B. licheniformis* (dark blue), human pancreas (orange), and *Tenebrio molitor* (in pink). (d) Superposition of β-strand 7 through α-helix 7 of the $(\beta/\alpha)_8$-barrel domain from family 13 members with different specificities: AMY2 (red), *Ps. stutzeri* maltotetraohydrolase (dark blue), *Ps. amyloderamosa* isoamylase (pink), *T. vulgaris* R-47 α-amylase II (orange), *B. cereus* oligo-1,6-glucosidase (green), and *B. circulans* cyclodextrin glycosyltransferase (light blue). In panels c and d, the starting residue is the first of β-strand 7 and the last residue is at the C-terminus of α-helix 7.

out an rms fit between all C_α atoms within a distance of 0.3 Å further increased to 1 Å. The compared structures comprise the following α-amylases (PDB entry codes in parentheses): *A. niger* (2AAA), *Ps. haloplanktis* (1AQH and 1B0I), yellow meal worm (1JAE), barley AMY2 (1AMY and 1BG9), HPA, human pancreas (1HNY), *A. oryzae* (6TAA and 7TAA), and *B. licheniformis* (1BLI). The compared structures also comprise the following different family 13 enzymes: *Pseudoalteromonas stutzeri* maltotetraohydrolase (2AMG), TVAII, *Thermoactinomyces vulgaris* R-47 α-amylase II (1BVZ), *Pseudoalteromonas amyloderamosa* isoamylase (1BF2), *Bacillus cereus* oligo-1,6-glucosidase (1UOK), *Bacillus circulans* strain 8 cyclodextrin glycosyltransferase (1CGT), and barley AMY2 (1AMY and 1BG9).

RESULTS

Choice of the $F^{286}VD$ Target Sequence. Glycoside hydrolase family 13 of amylolytic and related enzymes has very low degree of sequence identity (*2*, *4*, *37*). Thus, only three catalytic acids, two histidines binding substrate at subsite −1 and an aspartic acid−arginine salt bridge stabilizing the active site geometry, are invariant (*4*, *13*, *50*). Binding of acarbose at subsites −1 through 2 in barley AMY2 (Figure 2a,b) involves some of these residues and residues in sequence motifs at $\beta \rightarrow \alpha$ loops 3 (i.e., domain B), 4, and 5 of the catalytic $(\beta/\alpha)_8$-barrel (*21*) associated with specificity (*2*, *4*, *56*).

Via superpositioning of the three catalytic acids, the excellently shared conformation of β-strand 7 Lys282−Thr285 sequence (AMY1 numbering is used throughout in the text) and its immediate extension, the conserved Phe286−Asp288 sequence (the mutagenesis target, see below and Figure 3), were presented for seven α-amylases (Figure 2c) and five other family members (Figure 2d). This structure comparison in addition highlighted the contrasting diversity at the C-terminal part of $\beta \rightarrow \alpha$ segment 7, Thr292−Gly316, that succeeds a 3_{10}-helix, Asn289−Asp291, carrying the essential Asp291 and His290, and the conserved Asn289 bridged by a water molecule to Asp291, in turn bridged to the proton donor Glu205 by another water molecule (*21*, *22*). Notably, His305 ND1 (not indicated) in the corresponding C-terminal region of $\beta \rightarrow \alpha$ segment 7 rearranged from subsite 1/2 in free porcine and human pancreatic α-amylases to form a hydrogen bond with glucosyl O(2) of a bound acarbose-type inhibitor at subsite −2, accompanied by a main chain movement of 3.5−5 Å (*28*, *29*, *48*). A similar interaction has not been reported for Taka-amylase A (*26*) or cyclodextrin glycosyltransferase (*39*) which bound acarbose derivatives to subsites −3 through 3 or subsites −7 through 2, respectively, or by binding maltotetraose at subsites −1 through −4 in maltotetraohydrolase (*51*). But the short substrate maltopentaose was bound at subsites −3 through 2 in an inactive catalytic site mutant of *B. subtilis* α-amylase (*34*), and although a rearrangement was not reported, interestingly in this enzyme ND2 of Asn273 from the variable part of $\beta \rightarrow \alpha$ segment 7 was within hydrogen bonding distance of glucosyl O(2) at subsite −2, reminiscent of the His305 interaction (*34*).

The choice to alter the $F^{286}VD$ sequence in AMY1 was based on its conservation (Figure 3). This decision ties with the role of $\beta \rightarrow \alpha$ segments in specificity and substrate binding and in particular with the C-terminal part of $\beta \rightarrow \alpha$ segment 7 being highly variable and, as described above, interacting with substrate at the glycon binding region in some enzymes. The present target sequence was restricted to $F^{286}VD$ in light of earlier successful random mutation of $R^{183}GY$ in $\beta \rightarrow \alpha$ loop 4, as opposed to the longer target Arg183−Glu188 sequence being futile (*14*) probably partly because of the limited number of transformants which could be screened relative to the number of possible sequence combinations (*66*) and partly because of the hexapeptide target encompassing certain structural constraints.

Certain mutations of the $F^{284}VD$ sequence in AMY2 (AMY1 $F^{286}VD$) in silico created structural conflicts. Therefore, to achieve a convenient frequency of functional mutants, a biased random mutagenesis protocol (Table 1 and Figure 1) was implemented on the basis of family 13 tripeptide sequences selected from α-amylases, exo-α-amylases, α-glucosidases, pullulanases, isoamylases, neopullulanases, and glucosyltransferases (for examples, see Figure 3). The designed primers theoretically encode 174 $F^{286}VD$ mutants. These include a few rare or novel sequences featuring His or Gln at position 286, Arg or Gly at position 287, and Lys, Arg, or Gly at position 288, while the naturally occurring Ile or Thr matching Val287 (Figure 3) was disallowed to avoid primers for mutant genes encoding eight extra amino

Enzyme	Species	Stretch from β7→α7	Accession Number	Crystal structure refs.
		β β β L L L h h h B C		
α-Amylase				
	Hordeum vulgare (AMY1)	A A T **F V D** N H D	J01236	
	Hordeum vulgare (AMY2)	A V T **F V D** N H D	K02637	21,22
	Triticum aestivum (Wheat3)	T V T **F I D** N H D	X05809	
	Mung bean	A V T **F I D** N H D	X73301	
	Human pancreas	A L V **F V D** N H D	P04746	28,29
	Yellow meal worm	A V V **F V D** N H D	P56634sp	32
	Aspergillus oryzae	L G T **F V E** N H D	D00434	25,26
	Aspergillus niger	L G N **F I E** N H D	P56271	27
	Pseudoalterom. haloplanktis	A V V **F V D** N H D	P29957	36,54,68
	Bacillus licheniformis	A V T **F V D** N H D	X03236	33
	Saccharomycopsis fibuligera	L T N **F V E** N H D	X05791	
α-Glucosidase	*B. stearothermophilus*	N A L **F L E** N H D	D84648	
Maltotetraohydrolase	***Pseudomonas stutzeri***	A V T **F V D** N H D	M24516	41,51
Maltohexaohydrolase	*Bacillus* sp. 707	A V T **F V D** N H D	M18862	
Pullulanase	*Klebsiella pneumonia*	V V N **Y V S** K H D	X52181	
Pullulanase (limit dextrinase)	*Hordeum vulgare*	T I N **Y V S** A H D	AF022725	
Isoamylase	***Pseudomonas amyloderamosa***	S I N **F I D** V H D	M25247	42
	Hordeum vulgare	S I N **F V C** A H D	AF142589	
Amylopullulanase	*Bacillus cereus*	L M N **L I G** S H D	D28467	
Neopullulanase	*B. stearothermophilus*	A F N **L L G** S H D	Z94043	
Neopullulanase-α-amylase	*Thermoact.* vulg. R-47-I	M M N **F L S** N H D	D13177	
	Thermoact. vulg. R-47-II	L W N **L L D** S H D	D13178	43
Cyclomaltodextrinase	*Thermus* sp. IM6501	A F N **L L G** S H D	O69007	44
Dextran glucosidase	*Streptococcus mutants*	N S L **F W N** N H D	M77351	
Oligo-1,6-glucosidase	***Bacillus cereus***	N S L **Y W N** N H D	X53507	40
Branching enzyme	*E. coli*	T E N **F V L**(PL)N H D	M13751	
	Hordeum vulgare	C V T **Y A E** S H D	AF064560	
Cyclodextrin glycosyltransferase	***Bacillus circulans* strain 8**	Q V T **F I D** N H D	X68326	39,50
Amylomaltase	*Streptococcus pneumonia*	S V M **Y T G** T H D	J01796	
	Potato	Q V V **Y T G** T H D	X68646	

FIGURE 3: Sequence alignment of $\beta \rightarrow \alpha$ segment 7 in glycoside hydrolase family 13. Tripeptides equivalent to the target F[286]VD sequence in barley AMY1 are in bold. β, L, and h designate β-strand, loop, and 3_{10}-helix in the AMY2 structure (*22*), respectively. B designates a substrate binding and C a catalytic residue (*21*, *22*). Enzymes in bold are used in panels c and d of Figure 2.

Table 2: Identified Mutations in the F[286]VD Sequence of C95A-AMY1

mutant	yield (μg/L)	comments on mutant structure accommodation[a]
FVG	1.0, active	excellent; Asn291 and His290 become flexible; the Lys251−Asp288 salt bridge is lost
FGG	3.0, active	good; Asn291 and His290 become highly flexible; disturbs clusters of Phe301 and Tyr310, and Trp299, Trp207, Phe248, and Phe246
FLE	3.4, active	poor; Glu288 clashes with Thr290 (not shown) and is close to Lys251 NZ; Glu288 and Leu287 require backbone movement
YVD	1.7, active	poor; Tyr286 is very close to Phe248 and affects an aromatic cluster
LLD	0.9, active	acceptable; Leu286 weakens aromatic cluster and water pocket interactions; Leu287 is too close to Tyr310, but may rotate
FWG	1.4, inactive	poor; Trp287 is too close to Tyr310 and/or Phe301 and/or His326
FLD/FFD	nf[b]	poor; Leu287/Phe287 is too close to Val306 and/or Phe301 and/or His326; Leu287 is not free to rotate, and Phe287 is close to Tyr310
FVN/FLN/FLS	nf[b]	poor; the Lys251−Asp288 salt bridge is lost
FFN/FRN	nf[b]	bad; Phe287/Arg287 is too close to Tyr310 and/or Phe301 and/or His326 and/orVal306; the Lys251−Asp288 salt bridge is lost
FGN	nf[b]	bad; cluster of Tyr310 and Phe301 and the Lys251−Asp288 salt bridge are lost
HVE/YGE	nf[b]	bad; His286/Tyr286 is too close to Phe248 and perturbs the cluster of Phe246, Phe248, and Trp207; Glu288 is too close to Lys251 NZ
QLD/LLE	nf[b]	bad; Gln286/Leu286 causes loss of the aromatic cluster; Leu287 is too close to Tyr310 and requires conformational change; Glu288 is too close to Lys251 NZ
LEG	nf[b]	bad; Glu287 clashes with His326
ΔWD	nf[b]	bad; destroys aromatic cluster of Phe248, Trp207, Trp299, and Phe246
ΔΔR	nf[b]	very bad; only accommodated with major disruption of tertiary structure

[a] See Figures 4 and 5 for local interactions. [b] Not formed.

acids at this position, including Cys and Pro which could severely perturb the protein structure.

Production of F[286]VD Mutants of C95A-AMY1. As the parent enzyme for the production of FVD mutants was used C95A-AMY1 to avoid inactivating glutathionylation of AMY1 Cys95 by the host (*11*, *14*), and the FVD mutants have not been produced in the wild-type protein. The obtained frequency of encoded FVD mutants was approximately 25%, and *S. cerevisiae* was transformed using 21 isolated clones of 5 single, 11 double, and 5 triple replacements in F[286]VD (Table 2). These included cases of all planned residues, Phe, Leu, Tyr, His, or Gln, at position 286 (Table 1), of which the three former occurred in active variants (Table 2). Likewise, mutant genes for all planned replacements at position 287 were obtained, of which Val, Gly, and Leu occurred in active mutants and Trp in an inactive mutant (Table 2). At position 288, Asp, Glu, and Gly, but not Asn or Ser, were represented in active mutants and no isolated genes encoded Lys or Arg. No protein was detected containing the deletion ΔWD and ΔΔR mutations (Table 2), which probably arose due to the lack of Taq polymerase proofreading. Mistranscription could also explain formation of unintended genes encoding FFN, FFD, and LEG.

Colonies of *S. cerevisiae* transformants harboring FVG, FGG, FLE, LLD, and YVD mutant plasmids formed small

Table 3: Enzymic Properties of $F^{286}VD$ Mutants of C95A-AMY1[a]

	Blue Starch	Cl-PNPG$_7$			amylose DP17			relative specificity	
enzyme	activity (units/mg)	k_{cat} (s^{-1})	K_m (mM)	k_{cat}/K_m (mM^{-1} s^{-1})	k_{cat} (s^{-1})	K_m (mg/mL)	k_{cat}/K_m (mL mg^{-1} s^{-1})	Blue Starch:Cl-PNPG$_7$ [units/mg (k_{cat}/K_m)]	amylose DP17:Cl-PNPG$_7$ [(k_{cat}/K_m):(k_{cat}/K_m)]
C95A-AMY1	4000	75	9.8	7.7	464	2.2	211	520	27
FVG	1950	58	3.5	17	47	0.7	67	115	3.9
FGG	375	32	1.1	29	48	0.7	69	13	2.4
YVD	705	6.2[b]	1.5	4.1	29[b]	0.5	58	172	14
FLE	21	4.9	5.7	0.9	5.6	1.5	3.7	23	4.1
LLD	144	4.0	1.9	2.1	11	0.4	28	69	13
rAMY1	2500	119	1.7	70	165	0.6	275	36	3.9

[a] In general, kinetic parameters are averages of three experiments varying within ±15%. [b] The value is corrected due to the low stability for loss (≤50%) in activity since the level of purification was based on activity toward insoluble Blue Starch measured at the time of the kinetics analysis.

halos on starch plates. The corresponding functional enzymes were purified from preparative-scale cultures and gave one band on SDS−PAGE; the isoelectric points (not shown) suggested that they were of the full-length AMY1 form (*11*). Thus, the substantial trimming of a few C-terminal amino acid residues in C95A and wild-type rAMY1 produced by *S. cerevisiae*, which characteristically decreased the isoelectric point (*11*), was negligible for the FVD variants, perhaps due to their low secretion level. Immunoblots of lysed cells (not shown) indicated an intracellular FWG variant at ∼100 times the secreted amount. Also, the FVG variant was present partly inside the cells. As wild-type rAMY1 did unfold irreversibly (*67*), no effort was made to recover variants from the cells. Finally, protein corresponding to any of the 15 remaining mutant genes was detected neither in the medium nor intracellularly (Table 2).

Although C95A-AMY1 transformant cultures contained 5−20 mg/L, the $F^{286}VD$ mutants reached a concentration of only 0.9−3.4 μg/L (Table 2). As *P. pastoris*, however, secreted 20−100 mg/L wild-type rAMY1 (*12*) and formed large halos on starch agar plates after 12−15 h, this host was tested with seven selected (see below) mutants genes in an attempt to improve the amounts. But only small halos appeared on starch plates around colonies after 4 days. *P. pastoris* thus secreted FVG, FGG, and LLD mutants at 1.0−10 μg/L and the unstable YVD at 50 μg/L, while FLN, FLS, and ΔWD mutants were not obtained. As both yeast hosts thus produced ≤0.1% of the variants compared to the C95A parent or wild-type AMY1, mutations of FVD seemed to elicit difficulties in folding, secretion, and/or stability. In fact, depending on the concentration, the YVD mutant lost up to 90% activity at 4 °C within 3 days of purification, whereas other FVD mutants, C95A-AMY1, and wild-type rAMY1 retained activity for at least several weeks. Thorough characterization of the conformational stability was not possible because of the small amount of the variants that was available.

Enzymatic Properties of $F^{286}VD$ Mutants. A small collection of two single and three double functional FVD mutants was obtained, and overall, the FVG and FGG mutants displayed the best activity (Table 3). All five mutants had significantly improved affinity, and their k_{cat} values varied from being essentially retained to having decreased by 2 orders of magnitude relative to that of the parent enzyme, C95A-AMY1. The activity range covered by the variants for insoluble Blue Starch was more than twice as large as the ranges for the two soluble substrates (Table 3), and while only the parent enzyme displayed high activity compared to wild-type rAMY1 toward Blue Starch, all variants for the two soluble substrates showed superior affinity as indicated by the K_m values (Table 3).

In hydrolysis of Cl-PNPG$_7$ and amylose DP17, K_m values of the mutants were 1.5−8.9 times lower than of the parent C95A-AMY1 and they remarkably resembled those of wild-type rAMY1. Mutation of the $F^{286}VD$ sequence, located near subsites 1/2, apparently compensated for the adverse effect on substrate binding by the strategic C95A substitution at subsites −5/−6 (*14*, *24*). In contrast, C95A-AMY1 had activity toward insoluble Blue Starch being 2−200-fold superior to those of the five different mutants and 1.6-fold superior to that of wild-type rAMY1.

The catalytic efficiency, k_{cat}/K_m, for Cl-PNPG$_7$ was 380 and 220% for FGG- and FVG-AMY1 of C95A-AMY1, respectively, but only 33% toward amylose (Table 3). While the k_{cat} values for Cl-PNPG$_7$ of the FVG and FGG mutants were 42 and 77%, respectively, values of 4−6% of C95A-AMY1 were obtained for the FLE, LLD, and YVD mutants. In the case of the YVD mutant, the measured low activity may have been caused partly by its instability. k_{cat} for amylose was lower, i.e., 7−10% for the FVG, FGG, and YVD and only 1−2% for the FLE and LLD mutants compared to that of the parent enzyme. The effect of the mutations was thus highly differentiated by the substrates as illustrated also by the wide ranges of 13−172 and 2.4−14 for the calculated relative specificities of the starch−oligosaccharide and amylose−oligosaccharide combinations, respectively. The parent's values of 520 and 27 reflected its particularly low and high catalytic efficiencies (k_{cat}/K_m) toward Cl-PNPG$_7$ and amylose, respectively (Table 3). Compared to the parent, the FGG mutant thus favored by 40-fold the hydrolysis of Cl-PNPG$_7$ over that of insoluble Blue Starch, while intermediary values were found for the other mutants and wild-type rAMY1. Although a less broad range was covered by the amylose:Cl-PNPG$_7$ specificity ratios, the trend for the relation between the FVD variant and parent enzymes was the same. The most and least active variants, containing FVG, FGG, and FLE, gave the smallest amylose:oligosaccharide specificity ratios, while the two with relatively favorable action on amylose, YVD and LLD, notably contained the wild-type Asp288 (Table 3). The YVD variant probably represented a case of substrate-mediated stabilization as it exhibited reasonable activity for amylose and insoluble starch, but not for Cl-PNPG$_7$.

Bond Cleavage Frequency Analysis for the FVG Mutant. Sets of productive binding modes of maltooligosaccharides were deduced from analysis of the relative substrate bond

Table 4: Bond Cleavage Frequencies in $PNPG_7$, $PNPG_6$, and $PNPG_5$ Hydrolyzed by the FVG Variant and Reference Enzymes

Enzyme	Relative cleavage frequency (%)	Cleaved substrate (%)	[E] (nM)	Time (min)	Relative rate[d] (%)
	G - G - G - G - G - G - G - PNP				
F^{286}VG-mutant	16 75 9	9.3	80	0.5	100
C95A-AMY1[a]	88 12	2	280	0.5	6
rAMY1[b]	93 7	12	7	1.8	420
AMY2[c]	95 5	n.d.	170	0.3	n.d.
	G - G - G - G - G - G - PNP				
F^{286}VG-mutant	14 9 16 20 41	11	80	5	100
C95A-AMY1[a]	20 76 5	9.9	280	3	37
rAMY1[b]	1 18 29 52	13	67	2.8	250
AMY2[c]	21 19 18 14 28	n.d.	310	0.7	n.d.
	G - G - G - G - G - PNP				
F^{286}VG-mutant	66 27 7	9.5	80	11	100
C95A-AMY1[a]	21 40 39	4.3	280	5	28
rAMY1[b]	15 42 42 1	9.9	140	28	23
AMY2[c]	61 26 13	n.d.	510	1	n.d.

[a] Prepared as described in ref *14*. [b] Prepared as described in ref *12*. [c] Data from ref *18*. [d] Relative rates are estimated from the substrate consumption, enzyme concentration, and reaction time.

cleavage frequencies. FVG-AMY1 was selected for detailed characterization as it possessed high activity for the oligosaccharides and had good stability (Table 4). To suppress possible transglycosylation reactions, the decided concentration and consumption of substrate were $\leq {}^1/_{10}K_m$ and $\leq 13\%$, respectively. Indeed, transglycosylation products were not observed. Comparison of bond cleavage patterns of $PNPG_6$ and $PNPG_5$ indicated that FVG, C95A, and wild-type rAMY1 had distinctly different substrate binding mode preferences.

Subsite −6 in AMY1 has high affinity (*18*), and productive binding therefore tends to include interaction at that area if allowed by the substrate size, as was the case for $PNPG_6$ and $PNPG_7$. The major products from hydrolysis of $PNPG_6$ and $PNPG_7$ by FVG and wild-type AMY1 were 4-nitrophenol and PNPG, reflecting the interaction with subsite −6 (Table 4), whereas only 5% of the productive complexes of $PNPG_6$ occupied subsite −6 when Cys95 near subsite −5/−6 was replaced with Ala. Release of $PNPG_2$ from $PNPG_7$ by the FVG mutant showed that, exceptionally, 16% of the productive complexes covered subsites −5 through 2/3 and in addition 9% occupying subsites −7 through 1, whereas the dominant mode involved subsites −6 through 1/2. Thus, the mutant has a less firmly defined preferred binding mode. In contrast, $PNPG_7$ binding at subsites −5 through 2/3 was not applied by either parent or wild-type rAMY1 (Table 4). Together, these findings indicated that the mutation at FVD counteracted the adverse effect of the C95A replacement. The results suggested that interactions with the substrate aglycon part were enhanced by the mutation as a larger proportion of longer hydrolysis products, $PNPG_n$, was produced compared with both wild-type rAMY1 and C95A-AMY1 (Figure 4). This was particularly obvious with the shorter substrate $PNPG_5$ from which the mutant releases mainly $PNPG_3$, whereas PNPG and $PNPG_2$ constituted 80−85% of the products generated by C95A-AMY1 and wild-type rAMY1. $PNPG_5$ was too short to bind at subsite −6 in the productive mode, and the C95A substitution had a limited impact on the conversion of $PNPG_5$ as seen from the shared product profile and the very similar rates of hydrolysis of C95A and wild-type rAMY1 (Table 4). The higher rate of hydrolysis of $PNPG_5$ measured for the mutant compared to that for the reference enzyme forms (Table 4) supported the fact that particularly favorable effects of the FVG mutation appeared in reaction with short substrates. The action patterns for the AMY2 isozyme on $PNPG_5$ and $PNPG_6$ resembled those of the AMY1 FVG mutant but not of wild-type AMY1, demonstrating that natural structural variation can also change product profiles concurrent with retained activity levels.

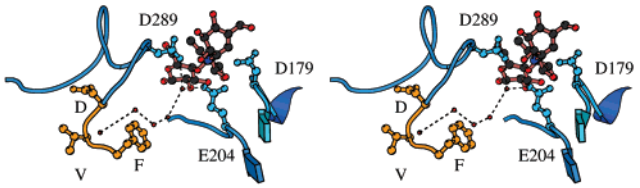

FIGURE 4: Stereodrawing highlighting interactions involving the entire FVD (orange) region of F^{284}−Gly^{291}, catalytic acids Asp179, Glu204, and Asp289 [AMY2 numbering (blue)], the water in a pocket (*21*), and acarbose. Wat607 (not labeled) is hydrogen bonding to Glu204 and Asp289. The corresponding residues in AMY1 are F^{286}−Gly^{293}, Asp180, Glu205, and Asp291.

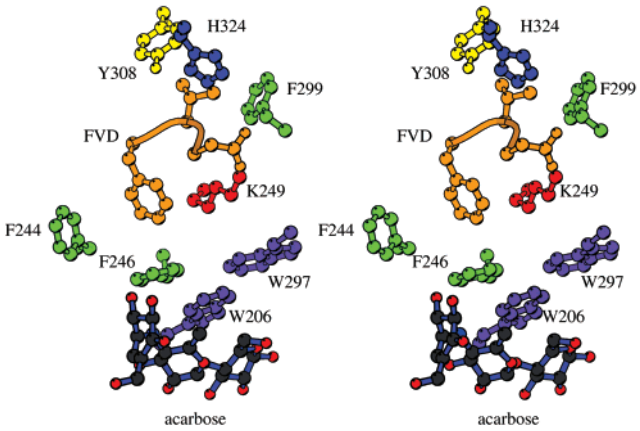

FIGURE 5: Closeup stereodrawing of AMY2/acarbose, including residues in the FVD surroundings which through aromatic/hydrophobic, hydrogen bond, and electrostatic interactions are likely to be affected by mutations and influence activity (AMY2 numbering). The corresponding residues in AMY1 are Trp207, Phe246, Phe248, Lys251, Trp299, Phe301, Tyr310, and His326.

DISCUSSION

The conserved F^{286}VD sequence from $\beta \rightarrow \alpha$ fragment 7 was demonstrated to be a valuable target for mutational manipulation of enzymic properties in barley α-amylase isozyme 1 (AMY1). Because the N- and C-terminal residues of FVD bridged secondary structure elements (Figures 2c,d and 4; *21*), it was envisaged that small structural variations would influence key functional residues through aromatic clusters, and hydrogen bond and electrostatic network interactions with relation to FVD (Figures 4 and 5), although FVD was not binding to acarbose (*21*). The effects of FVD mutations as discussed below therefore seemed problematical to grasp on a structural basis. FVD in addition lined a water-containing pocket involving two catalytic acids (Figure 4; *21*). The psychrophilic α-amylase contains an equivalent

water channel (*68*). It is unknown, however, if these water-filled cavities participated in the mechanism. No information is available on mutations of FVD counterparts in other members of glycoside hydrolase family 13.

Three FVD mutants, FVG, FGG, and YVD, had reasonable activity; two, FLE and LLD, exhibited lower activity, and one, FWG, had no detectable activity. This outcome was rationalized by evaluating the impact of the hypothetical sequence changes on the structure. As approximately 10^3 fold less FVD mutants were produced compared to both the C95A and wild-type AMY1 and two mutants, FVG and FWG, occurred intracellularly, secretion or folding may have been hampered. Although saturation of the chaperone folding machinery of the endoplasmic reticulum would normally cause cells to degrade misfolded protein to prevent aggregation (*69*, *70*), this apparently did not happen for the FVG and FWG mutants. It cannot be excluded, however, as the proper explanation for the 15 mutant genes that failed to lead to protein variants (Table 2). Earlier, the subtle modification in the catalytic residues of D180N and E205Q mutants resulted in production of 0.1−1% protein and 1−10% D291N (*13*) compared to wild-type AMY1 in *S. cerevisiae*. The H93N and H290N mutations of transition-state stabilizing residues and of W279A in a surface starch granule binding site (Figure 2a) were also obtained in 0.1% yield (*13*). Different variants of the $\beta \rightarrow \alpha$ loop 4 specificity motif ($R^{183}GY$) were made at 0.1−10% of the wild-type level (*14*), and recombinant wild-type AMY2 was secreted in approximately 1% yield of rAMY1 (*10*−*12*). Thus, several barley α-amylase forms were difficult to produce in yeast. It has not been possible to identify the origin of the low yields.

Variation and Structural Accommodation of FVD in Family 13. FVD was found in 13, FID in 8, and FLD in 1 of 22 plant α-amylase sequences, suggesting that conservative AMY1 variants would best retain function. The high activity of the FGG and FVG mutants therefore was unexpected. Interestingly, Gly was extremely rare in the target tripeptide and only reported in a *Micrococcus* α-amylase sequence and a *Streptomyces* α-amylase sequence, both having FLG. Gly was never seen to correspond to AMY1 Phe286 or Val287. This outcome of the biased random mutagenesis strongly advocates irrational generation of mutants coupled with a judicious choice of target sequence and a careful preselection of the candidate replacing residues.

The three less active YVD, FLE, and LLD mutants had known counterparts in *Streptococcus*, *Cryptococcus*, and *Bacillus* α-amylases, respectively. FLE also resembled FVE in Taka-amylase and FID in plant α-amylases, while LLD resembled LVD in a *B. stearothermophilus* α-amylase. Examples from other specificities in glycoside hydrolase family 13 included LLD in neopullulanase and cyclodextrinase, FID in isoamylase and cyclodextrin glycosyltransferases, and YVS in pullulanase. However, even though the AMY1 variant tripeptides resembled sequences in enzymes acting near or on α-1,6 linkages (pullulanase, isoamylase, oligo-1,6-glucosidase, neopullulanase, dextran glucosidase, and cyclomaltodextrinase), none of the present transformants [including the one producing the FWG variant (Table 2) resembling FWN in dextran glucosidase and YWN in oligo-1,6-glucosidase] hydrolyzed pullulan on agar plates, although the other five variants which were active toward starch also formed halos on amylopectin plates (T. E. Gottschalk and B. Svensson, unpublished observation).

The FVG and FGG substitutions reduced the negative charge. This would perturb the electrostatic field that stabilized oxacarbenium ion transition states at the active site, and the elevated pK_a of Glu205, the proton donor and acid/base catalyst, as described in the retaining mechanism characteristic of glycoside hydrolase family 13 (*21*, *50*, *71*). As FVG and FGG mutants had high activity for Cl-$PNPG_7$, the replacement of Asp288 was not critical. In silico mutations indicated highly increased flexibility of $\beta \rightarrow \alpha$ segment 7 in the FVG and FGG mutants, while certain other replacements, stressing the crucial role of FVD, were not properly integrated. Most remarkably, in a recent analysis of architectural key features stabilizing the $(\beta/\alpha)_8$-scaffold of family 13 (*72*), the C-terminal capping Phe286 in the VTF^{286} tripeptide from β-strand 7 (Figure 3) was exceptionally well conserved among the tripeptide sequences in each of the eight β-strands that played a role in the internal packing of the barrel β-sheet. FVD variants, however, are seen in related enzyme structures. Room for Trp in YWN in oligo-1,6-glucosidase was achieved by backbone shifts in the surroundings. A relative shift in the surroundings similarly incorporated LLD in TVAII α-amylase without clashing with the side chain equivalent to Tyr310 (AMY2 Tyr308; Figure 5). Whereas helix 7 was displaced in isoamylase and cyclodextrin glycosyltransferase having FID, the structure of maltotetraohydrolase, having FVD, was essentially as in AMY2. Although these enzymes possessing very little overall sequence identity showed excellent superpositioning of their secondary structure elements of the barrel fold, the observed local subtle changes in the surroundings in structures of related enzymes may not imply that analogous structure adjustments are possible in AMY1 FVD variants.

Replacement in $F^{286}VD$ with bulky groups generally created difficulties as was evident from inspection of the AMY2 structure. Thus, Glu288 would be too close to Lys251 (*21*, *22*), and the FLE mutant in fact was the least active of the five active variants. Furthermore, no protein was detected from one single, five double, and five triple mutant genes at position 288, including three having Glu288. Indeed, FVE in Taka-amylase A was accommodated by a position shift for helix 7 relative to AMY2. Asp288 OD2 in AMY1 (AMY2 Asp286) formed a salt bridge with Lys251 NZ (Figure 5; AMY2 Lys249), and the Lys side chain was in hydrophobic contact with Phe286 (AMY2 Phe284) belonging to a cluster, including Phe246 and Phe248, that stacked onto Trp207 and Lys251 (Figure 5; Phe244, Phe246, Trp205, and Lys249 in AMY2). Both this salt bridge and the hydrophobic cluster probably restricted changes in FVD, although they could not be essential as FVG- and FGG-AMY1 are highly active. Moreover, if the Lys251−Asp288 salt bridge was present in the unstable YVD-AMY1, it was unable to ensure conformational stability. The hydrophobic contacts of Phe286 thus seemed more critical than the salt bridge. In agreement with this interpretation, variants having His or Gln at position 286 were not formed. Remarkably, only Phe, which was predominant, Trp (not comprised by the present design of biased random mutagenesis primers), Tyr, and Leu occurred in α-amylases at this position which as mentioned above was important for the packing of the barrel β-sheet (*72*). Although Leu286 (AMY2 Leu284) was possible from a

geometric point of view, it would disturb both hydrophobic clusters involving wild-type Phe286 (Figure 5) and the internal barrel packing (*72*). Leu replacing Val287 would clash with Tyr310 (AMY2 Tyr308; Figure 5), and consequently, its conformation must be changed in the LLD mutant. Glu287 would come too close to His324 (Figure 5), which may be why the LEG mutant was not produced, despite the flanking Leu and Gly being found in functional mutants (Table 3). In fact, none of the five tested triple mutants were produced.

Enzymic Properties of FVD Mutants in Relation to Structural Features. The AMY1 variants represent dual-subsite substitution in which mutation of FVD near subsite 1/2 (Figure 2b) remarkably restored activity (k_{cat}/K_m) for short substrates and the substrate affinity (K_m), both being reduced by the parent C95A mutation at subsite −5/−6. F[286]VD was near the active site His290 and Asp291, both forming hydrogen bonds with acarbose at subsite −1 and participating in structural networks (*21*, *22*). As Asp291 maintained the elevated pK_a of the proton donor Glu205 and exerted strain on the substrate conformation at subsite −1 and a water molecule bridged Asp291 and Glu205 (Figure 4; *21*, *41*, *50*, *51*), mutations were anticipated to influence activity also through long-range perturbations in tertiary structure.

The activity toward insoluble starch amylose DP17 (that spans the 10 binding subsites in AMY1), and the shorter Cl-PNPG$_7$, reflected the distinctly different impact of FVD mutants on substrate interplay at different parts of the binding site. While affinity was generally improved for Cl-PNPG$_7$ and amylose, k_{cat}/K_m was increased for some mutants and only for Cl-PNPG$_7$. Replacement of Asp288 with Glu resulted in the highest K_m, although it was still lower than that of AMY1, probably due to Glu288 interfering with Thr290 and NZ of Lys251. The increased flexibility of FVG- and FGG-AMY1 did not enable activity enhancement when substrate filled the entire cleft, as k_{cat} values of mutants for Cl-PNPG$_7$, a rather poor substrate, and amylose were strikingly similar, while the single mutant C95A-AMY1 had a 5 times higher k_{cat} toward amylose. FVD mutation was thus relatively unfavorable for activity and for enzyme−substrate contacts a certain distance from the catalytic site. This implied that FVD was important in such interactions, although no structural details from modeling of AMY2/maltododecaose depicted such interactions (*24*), which have been described in a few α-amylases as movement upon substrate binding of the region encompassing FVD (*73*). The low activity toward starch of the FGG as compared to that of the FVG variant may stem from perturbation of several interconnected aromatic clusters (Figure 5). Wide variation in the substrate preference by the different enzyme forms was apparent from the starch:Cl-PNPG$_7$ and amylose:Cl-PNPG$_7$ specificity ratios, which changed by factors of 40 and 11, respectively. It is possible that different binding modes were applied to short and long substrates, in accordance with a small ensemble of maltodextrin docking solutions being computed for different α-amylases (*74*).

Substrate binding in α-amylases and related enzymes has been illustrated by crystal structures (*20*, *21*, *26*, *28*, *39*, *68*), and the shift of His305 in $\beta \rightarrow \alpha$ segment 7 in pancreatic α-amylase to bind inhibitor at subsite −2 (*28*, *29*, *48*) was confirmed to close the cleft in the active enzyme binding a nonhydrolyzable substrate analogue, methyl 4,4′-dithio-α-maltotrioside (*75*). The FVG mutant weakened glycon binding for PNPG$_7$ and PNPG$_5$, but restored the PNPG$_6$ interaction at subsite −6, from a level of 5% in C95A-AMY1 to a level of 41% in the mutant which was comparable to the level of 52% in wild-type AMY1. Evidently, there was a multifaceted functional connection between FVD and events at distant glycon binding subsites. The mutation may either improve interaction at subsites toward the reducing end, weaken glycon binding, or both. The small amount of mutant enzyme available and the high K_m (≥10 mM) for these substrates, however, prohibited experimental analysis of substrate affinity at individual subsites. No good structure-based explanation of the shift in PNPG$_6$ position can be offered here, but long-range interactions probably played a significant role. The question of whether $\beta \rightarrow \alpha$ segment 7 in AMY1 interacted with the substrate glycon like His305 (*28*, *29*, *48*) and Asn273 (*34*) in pancreatic and *B. subtilis* α-amylases, respectively, remains open. Only three-dimensional structures can show it, but the AMY2−acarbose complex displays protein−substrate interactions at only subsites −1 through 2 (*21*).

Conclusion. By application of a combined rational and irrational approach, genetic variants of barley α-amylase 1 with attractive and instructive enzymic properties were made. The generally enhanced affinity coupled with high activity toward oligosaccharides in the FVG and FGG variants was particularly interesting as Gly was essentially lacking at these positions in natural sequences. These findings build confidence in future gene shuffling and in vitro evolution studies for improvement of function.

Although high ligand affinity is generally an important goal in protein engineering, it has received little attention in amylolytic enzymes, most probably because high substrate concentrations are used in the majority of relevant enzyme-catalyzed processes. However, with the growing diversity of applications and the large number of enzyme specificities represented in family 13, improving affinity particularly for action on oligosaccharides becomes an asset. Indeed, although affinity as a rule is low for short maltooligosaccharides, it is amenable to amelioration by protein engineering as demonstrated by the present restoration mutations. The results also show the impact of substrate size possibly in controlling the dynamics of $\beta \rightarrow \alpha$ loop 7, as short substrates were comparatively easily converted by the FVG and FGG mutants with higher conformational flexibility. The critical effect on activity, however, apparently depended on whether specific parts of the binding cleft were free or occupied by substrate. The shared catalytic site geometry in family 13 coupled with structural diversity in $\beta \rightarrow \alpha$ connecting segments that created the extended binding site and defined the various substrate/product specificities made insights acquired in the present study applicable in engineering of other family members. It is emphasized that loop flexibility, which apparently was a valuable feature in $\beta \rightarrow \alpha$ segment 7, is a goal to be explored by engineering of FVD counterparts in related enzymes. As accentuated in this and other studies, after successfully engineering and gaining insight into thermostability determinants for groups of α-amylases (*4*, *73*), we enter the era of specificity engineering where much remains to be explored and understood. This should be achieved through exploitation of knowledge and analysis of mutant enzyme properties and available three-

dimensional structures, and use of recently developed procedures for creating and analyzing a library of structural diversity.

ACKNOWLEDGMENT

Annette J. Gajhede is thanked for technical assistance, Kristian S. Bak-Jensen for sharing the C95A-AMY1 bond cleavage data, and Bodil Corneliussen and Lone Sørensen for amino acid analyses.

REFERENCES

1. Yamamoto, T., Ed. (1995) *Enzyme Chemistry and Molecular Biology of Amylases and Related Enzymes*, The Amylase Research Society of Japan, CRC Press, Boca Raton, FL.
2. Svensson, B. (1994) *Plant Mol. Biol. 25*, 141−157.
3. Kuriki, T., Kaneko, H., Yanase, M., Takata, H., Shimada, J., Handa, S., Takada, T., Umeyama, H., and Okada, S. (1996) *J. Biol. Chem. 271*, 17321−17329.
4. MacGregor, E. A., Janecek, S., and Svensson, B. (2001) *Biochim. Biophys. Acta 1546*, 1−20.
5. van der Veen, B., Uitdehaag, J. C. M., Penninga, D., van Alebeek, G.-J., Smith, L. M., Dijkstra, B., and Dijkhuizen, L. (2000) *J. Biol. Chem. 296*, 1027−1038.
6. Parsiegla, G., Schmidt, A. K., and Schulz, G. E. (1998) *Eur. J. Biochem. 255*, 710−717.
7. Svensson, B., Mundy, J., Gibson, R. M., and Svendsen, I. (1985) *Carlsberg Res. Commun. 50*, 15−22.
8. Rogers, J. C. (1985) *J. Biol. Chem. 260*, 3731−3738.
9. Rogers, J. C., and Milliman, C. (1983) *J. Biol. Chem. 258*, 8169−8174.
10. Søgaard, M., and Svensson, B. (1990) *Gene 94*, 173−170.
11. Søgaard, M., Andersen, J. S., Roepstorff, P., and Svensson, B. (1993) *Bio/Technology 11*, 1162−1165.
12. Juge, N., Andersen, J. S., Tull, D., Roepstorff, P., and Svensson, B. (1996) *Protein Expression Purif. 8*, 204−214.
13. Søgaard, M., Kadziola, A., Haser, R., and Svensson, B. (1993) *J. Biol. Chem. 268*, 22480−22484.
14. Matsui, I., and Svensson, B. (1997) *J. Biol. Chem. 272*, 22456−22463.
15. Svensson, B., Bak-Jensen, K. S., Jensen, M. T., Sauer, J., Gottschalk, T. E., and Rodenburg, K. W. (1999) *J. Appl. Glycosci. 46*, 49−63.
16. Svensson, B., Bak-Jensen, K. S., Mori, H., Sauer, J., Jensen, M. T., Kramhøft, B., Gottschalk, T. E., Christensen, T., Sigurskjold, B. W., Aghajari, N., Haser, R., Payre, N., Cottaz, S., and Driguez, H. (1999) in *Recent Advances in Carbohydrate Bioengineering* (Gilbert, H. J., Davies, G. E., Henrissat, B., and Svensson, B., Eds.) pp 272−281, Royal Society of Chemistry, London.
17. Jones, R. R., and Jacobsen, J. V. (1991) *Int. Rev. Cytol. 126*, 49−88.
18. Ajandouz, E. H., Abe, J., Svensson, B., and Marchis-Mouren, G. (1992) *Biochim. Biophys. Acta 1159*, 193−202.
19. Robyt, J. F., and French, D. (1970) *J. Biol. Chem. 245*, 454−465.
20. Brzozowski, A. M., Lawson, D. M., Turkenberg, J. P., Bisgård-Frantzen, H., Svendsen, A., Borchert, T. V., Dauter, Z., Wilson, K. S., and Davies, G. (2000) *Biochemistry 39*, 9099−9107.
21. Kadziola, A., Søgaard, M., Svensson, B., and Haser, R. (1998)- *J. Mol. Biol. 279*, 205−217.
22. Kadziola, A., Abe, J., Svensson, B., and Haser, R. (1994) *J. Mol. Biol. 239*, 104−121.
23. Rodenburg, K. W., Juge, N., Guo, X.-J., Søgaard, M., Chaix, J.-C., and Svensson, B. (1994) *Eur. J. Biochem. 221*, 277−284.
24. André, G., Buléon, A., Haser, R., and Tran, V. (1999) *Biopolymers 50*, 751−762.
25. Matsuura, Y., Kusunoki, M., Harada, W., and Kakudo, M. (1984) *J. Biochem. 95*, 697−702.
26. Brzozowski, A. M., and Davies, G. J. (1997) *Biochemistry 36*, 10837−10845.
27. Boel, E., Brady, L., Brzozowski, A. M., Derewenda, Z., Dodson, G. G., Jensen, V. J., Petersen, S. B., Swift, H., Thim, L., and Wöldike, H. F. (1990) *Biochemistry 29*, 6244−6249.
28. Qian, M., Haser, R., Buisson, G., Duée, E., and Payan, F. (1994) *Biochemistry 33*, 6284−6294.
29. Machius, M., Vertesy, L., Huber, R., and Wiegand, G. (1996) *J. Mol. Biol. 260*, 409−421.
30. Ramasubbu, N., Paloth, V., Luo, Y., Brayer, G. D., and Levine, M. J. (1996) *Acta Crystallogr. D52*, 435−446.
31. Brayer, G. D., Luo, Y., and Withers, S. G. (1995) *Protein Sci. 4*, 1730−1742.
32. Strobl, S., Maskos, K., Betz, M., Wiegand, G., Huber, R., Gomis-Rüth, F. X., and Glockshuber, R. (1998) *J. Mol. Biol. 278*, 617−628.
33. Machius, M., Declerck, N., Huber, R., and Wiegand, G. (1998) *Structure 6*, 281−292.
34. Fujimoto, Z., Takase, K., Doui, N., Momma, M., Matsumoto, T., and Mizuno, H. (1998) *J. Mol. Biol. 277*, 393−407.
35. Dauter, Z., Dauter, M., Brzozowski, A. M., Christensen, S., Borchert, T. V., Beier, L., Wilson, K. S., and Davies, G. (1999) *Biochemistry 38*, 8385−8392.
36. Aghajari, N., Feller, G., Gerday, C., and Haser, R. (1998) *Protein Sci. 7*, 564−572.
37. Henrissat, B. (1991) *Biochem. J. 280*, 309−316.
38. Klein, C., and Schultz, G. E. (1991) *J. Mol. Biol. 217*, 737−750.
39. Uitdehaag, J. C. M., Kalk, K. H., van der Veen, B. A., Dijkhuizen, L., and Dijkstra, B. W. (1999) *J. Biol. Chem. 274*, 34868−34876.
40. Watanabe, K., Hata, Y., Kizaki, H., Katsube, Y., and Suzuki, Y. (1997) *J. Mol. Biol. 269*, 142−153.
41. Morishita, Y., Hasegawa, K., Matsuura, Y., Katsube, Y., Kubota, Y., and Sakai, S. (1997) *J. Mol. Biol. 267*, 661−672.
42. Katsuya, Y., Mezaki, Y., Kubota, M., and Matsuura, Y. (1998) *J. Mol. Biol. 281*, 885−897.
43. Kamitori, S., Kondo, S., Okuyama, K., Yokota, T., Shimura, Y., Tonuzuka, T., and Sakano, Y. (1999) *J. Mol. Biol. 287*, 907−921.
44. Kim, J. S., Cha, S. S., Kim, H. J., Kim, T. J., Ha, N. C., Oh, S. T., Cho, H. S., Cho, M. J., Kim, M. J., Lee, H. S., Kim, J. W., Choi, K. Y., Park, K. H., and Oh, B. H. (1999) *J. Biol. Chem. 274*, 26279−26286.
45. Przylas, I., Tomoo, K., Terada, Y., Takaha, T., Fujii, K., Saenger, W., and Sträter, N. (2000) *J. Mol. Biol. 296*, 873−886.
46. Feese, M. D., Kato, Y., Tamada, T., Kato, M., Komeda, T., Miura, Y., Hirose, M., Hondo, K., Kobayashi, K., and Kuroki, R. (2000) *J. Mol. Biol. 301*, 451−464.
47. Skov, L., Mirza, O., Henriksen, A., Potocki de Montalk, G., Remaud-Simeon, M., Sarbacal, P., Willemot, R.-M., Monsan, P., and Gajhede, M. (2001) *J. Biol. Chem. 276*, 25273−25278.
48. Brayer, G. D., Sidhu, G., Maurus, R., Rydberg, E. H., Braun, C., Wang, Y., Nguyen, N. T., Overall, C. M., and Withers, S. G. (2000) *Biochemistry 39*, 4778−4791.
49. Schmidt, A. K., Cottaz, S., Driguez, H., and Schulz, G. E. (1998) *Biochemistry 37*, 5909−5915.
50. Uitdehaag, J. C. M., Mosi, R., Kalk, K. H., van der Veen, B. A., Dijkhuizen, L., Withers, S. G., and Dijkstra, B. W. (1999) *Nat. Struct. Biol. 6*, 432−436.
51. Hasegawa, K., Kubota, M., and Matsuura, Y. (1999) *Protein Eng. 12*, 819−824.
52. Aghajari, N., and Haser, R. (1999) in *Recent Advances in Carbohydrate Bioengineering* (Gilbert, H. J., Davies, G. E., Henrissat, B., and Svensson, B., Eds.) pp 175−185, Royal Society of Chemistry, London.
53. Casset, F., Imberty, A., Haser, R., Payan, F., and Perez, S. (1995) *Eur. J. Biochem. 232*, 284−293.
54. Aghajari, N., Feller, G., Gerday, C., and Haser, R. (1998) *Structure 6*, 1503−1516.
55. Janecek, S., Svensson, B., and Henrissat, B. (1997) *J. Mol. Evol. 45*, 322−331.
56. Jespersen, H. M., MacGregor, E. A., Henrissat, B., Sierks, M. R., and Svensson, B. (1993) *J. Protein Chem. 12*, 791−805.

57. Juge, N., Rodenburg, K. W., Guo, X.-J., Chaix, J.-C., and Svensson, B. (1995) *FEBS Lett. 363*, 299−303.
58. Rodenburg, K. W., Vallée, F., Juge, N., Guo, X.-J., Aghajari, N., Haser, R., and Svensson, B. (2000) *Eur. J. Biochem. 267*, 1019−1929.
59. Gough, J. A., and Murray, N. E. (1983) *J. Mol. Biol. 166*, 1−19.
60. Sambrook, J., Fritsch, E. F., and Maniatis, T. (1989) *Molecular Cloning: A Laboratory Manual*, 2nd ed.; Cold Spring Harbor Laboratory Press, Plainview, NY.
61. Doyle, T. (1993) Ph.D. Thesis, Oxford University, Oxford, U.K.
62. Søgaard, M., Olsen, F. L., and Svensson, B. (1991) *Proc. Natl. Acad. Sci. U.S.A. 88*, 8140−8144.
63. Fox, J. D., and Robyt, J. F. (1991) *Anal. Biochem. 195*, 93−96.
64. Berman, H. M., Westbrook, J., Feng, Z., Gilliland, G., Bhat, T. N., Weissig, H., Shindyalov, I. N., and Bourne, P. E. (2000) *Nucleic Acids Res. 28*, 235−242.
65. Roussel, A., and Cambillau, C. (1991) in *Silicon Graphics Geometry Directory 86*, Silicon Graphics, Mountain View, CA.
66. Reidhaar-Olson, J. F., Bowie, J. U., Breyer, R. M., Hu, J. C., Knight, K. L., Lim, L. A., Mossing, M. C., Parsell, D. A., Shoemaker, K. R., and Sauer, R. T. (1991) *Methods Enzymol. 208*, 564−586.
67. Jensen, M. T. (1998) M.Sc. Thesis, University of Roskilde, Roskilde, Denmark.
68. Aghajari (1998) Ph.D. Thesis, Université de la Méditerranée Aix-Marseille II and Université de Liège, Marseille, France.
69. Rothman, J. E., and Orci, L. (1992) *Nature 355*, 409−415.
70. Rothblatt, J., Novick, P., and Stevens, T. H. (1994) *Secretory Pathway. A Sambrook & Tooze Publication*, Oxford University Press, Oxford, U.K.
71. McCarter, J. D., and Withers, S. G. (1994) *Curr. Opin. Struct. Biol. 4*, 885−892.
72. Pujadas, G., and Palau, J. (2001) *Mol. Biol. Evol. 18*, 38−54.
73. Nielsen, J. E., and Borchert, T. V. (2000) *Biochim. Biophys. Acta 1543*, 253−274.
74. André, G., and Tran, V. (1999) in *Recent Advances in Carbohydrate Bioengineering* (Gilbert, H. J., Davies, G. E., Henrissat, B., and Svensson, B., Eds.) pp 165−174, Royal Society of Chemistry, London.
75. Qian, M., Spinelli, S., Driguez, H., and Payan, F. (1997) *Protein Sci. 6*, 2285−2296.

BI0108608